

CHAPTER 30

Verification of numerical wave propagation models in tidal inlets

J.A. VOGEL, A.C. RADDER AND J.H. DE REUS*

The performance of two numerical wave propagation models has been investigated by comparison with field data. The first model is a refraction-diffraction model based on the parabolic equation method. The second is a refraction model based on the wave action equation, using a regular grid. Two field situations, viz. a tidal inlet and a river estuary along the Dutch coast, were used to determine the influence of the local wind on waves behind an island and a breaker zone. It may be concluded from the results of the computations and measurements that a much better agreement is obtained when wave growth due to wind is properly accounted for in the numerical models. In complicated coastal areas the models perform well for both engineering and research purposes.

1. INTRODUCTION

Sea waves approaching coastal regions can be influenced by a number of physical processes: shoaling, refraction by depth and current variations, diffraction, nonlinear effects, energy dissipation by wave breaking and bottom friction, and wave growth due to wind. In order to estimate inshore wave conditions from wave data available offshore, shallow water wave models should be able to account for these effects. Usually, numerical 2D shallow water wave propagation models include propagation and dissipation processes, while the influence of the local wind is often neglected (see e.g. Martin et al., 1987; Vincent and Carrie, 1988). For regions behind an island (c.q. peninsula) or a breaker zone the input from the local wind may be appreciable, and this effect cannot be accounted for by, e.g., taking a lower value of the friction factor. The purpose of this study is to verify two numerical models in this respect, with wave measurements in two field situations.

*senior researchers, Rijkswaterstaat, Tidal Waters Division,
P.O.Box 20904, 2500 EX The Hague, The Netherlands

2. SHALLOW WATER WAVE MODELS

The performance of two shallow water wave models has been investigated:

- The model CREDIZ, which is based on the parabolic approximation of the mild-slope equation (Radder, 1979; Dingemans et al., 1984; Dingemans 1985).
- the model HISWA, which is based on refraction computations using a regular grid (Holthuijsen and Booij, 1986; Holthuijsen et al., 1988)

A mathematical formulation of these models is given below.

2.1 THE MODEL CREDIZ

The parabolic model CREDIZ describes the propagation of waves in coastal areas with non-uniform depth and current, in particular where both refraction and diffraction effects are important. The model is based on the following equation for monochromatic wave motion (for more details, see Dingemans, 1985):

$$(1) \quad \nabla \cdot (cc_g \nabla \varphi) + (k^2 cc_g + i\sigma(W + \nabla \cdot \vec{U}))\varphi = 0$$

where \vec{U} is the (steady) current-velocity vector, ∇ is the horizontal gradient operator ($\partial/\partial x$, $\partial/\partial y$), $\varphi(x, y)$ is the complex wave potential function, k the wave number, c and c_g the phase- and group velocity, σ the relative angular frequency, $i = \sqrt{-1}$ the imaginary unit, and W a dissipation coefficient, to be specified later on.

The absolute (ω) and relative (σ) frequencies are related by:

$$(2) \quad \omega = \sigma + \vec{k} \cdot \vec{U}$$

where σ is given by the linear dispersion relation:

$$(3) \quad \sigma^2 = gk \tanh kh$$

with g the acceleration of gravity and h the local depth.

In the parabolic approximation the assumption is made that the waves propagate mainly into a specific direction, say x .

Defining the operator M by $M = \frac{\partial}{\partial y}(\beta \frac{\partial}{\partial y})$ with $\beta = cc_g$

the parabolic approximation to equation (1) is given by:

$$(4) \quad \frac{\partial}{\partial x}(\sqrt{\beta k} \varphi + \frac{p_1}{k \sqrt{\beta k}} M \varphi) - i(k \sqrt{\beta k} \varphi + \frac{p_2}{\sqrt{\beta k}} M \varphi) +$$

$$+\frac{\sigma}{2\sqrt{\beta k}}(W + \nabla \cdot \vec{U})\varphi = 0$$

The coefficients p_1 and p_2 result from the approximation of pseudo-operators by differential operators and are related by:

$$(5) \quad p_2 = p_1 + \frac{1}{2}, \quad 0 \leq p_1 \leq \frac{1}{2} \quad (\text{optimal : } p_1 = \frac{1}{4})$$

As the wave-number vector \vec{k} in (2) is not exactly known beforehand, the relative frequency σ is approximated by:

$$\sigma = \omega - r k U_x$$

in which r is a reduction factor expressing the fact that the waves do not exactly follow the x-direction ($0 \leq r \leq 1$; standard value: $r = 0.9$).

The energy-dissipation term $W\varphi$ in equation (4) accounts for the effects of wave breaking, bottom friction and wave growth due to wind:

$$(6) \quad W\varphi = (W_b + W_f + W_g)\varphi$$

The dissipation function W_b due to wave breaking is computed according to the method of Battjes and Janssen (1978); see also Battjes and Stive (1985). For the dissipation function W_f due to bottom friction the method of Putnam and Johnson (1949) is used.

The effect of wave growth by wind is simulated by the (negative) dissipation term W_g :

$$(7) \quad W_g = - \frac{2c_g}{H_s} \frac{dH_s}{dx}$$

where $H_s = 2a$ is the significant wave height and a the wave amplitude. To compute the gradient dH_s/dx in (7), the growth curve of Krylov/Wilson is used (cf. Holthuisen, 1980; Krylov et al.,1976; Wilson, 1965):

$$(8) \quad \tilde{H}_s = \beta [1 - 1 / (1 + \alpha \sqrt{\tilde{x}})^2]$$

with $\tilde{H}_s = gH_s / V_x^2$, $\tilde{x} = gx / V_x^2$,
 V_x = component of wind speed in x-direction,
 α, β = coefficients ($\alpha \approx 0.006$, $\beta \approx 0.256$).

It is noted that the growth curve (8) is based on a parametric description of the wave spectrum; the effect of wave growth is assumed to be local, while

the period of the waves (due to the restriction to monochromatic waves) is assumed to be constant, equal to the peak period of the spectrum. Therefore, a spectral decomposition is not allowed when (8) is used.

The influence of the wave amplitude a on the propagation velocity is taken into account by setting the local depth h in the dispersion relation (3) equal to: $h = d + p_v a$ where d is the actual mean water depth and p_v is an adjustable parameter (standard value: 1). In the shallow water limit the celerity c of a solitary wave is obtained for $p_v = 1$, while in the deep water limit the linear expression for c is recovered.

The parabolic differential equation (4) can be solved in finite difference form, using a two-level, implicit numerical scheme on a rectangular grid. When dissipative physical effects are included (through the term $W\varphi$), the difference equations are linearized in a special way to ensure stability: in the case of $W < 0$, a positive diffusion is introduced in the (fully implicit) numerical scheme, in order to prevent non-linear instabilities in the early stage of wave growth due to wind. In practice, fairly accurate solutions have been obtained for values of grid spacings Δx and Δy according to: $\Delta x/L \leq 1/4$; $\Delta y/L \leq 1/6$, where $L = 2\pi/k$ is the local wave length.

The solution of equation (4) requires as initial conditions the amplitude, period and direction of the incident wave field; along the lateral boundaries, the wave field is generally not known, and an approximate boundary condition (reflecting or partially absorbing) may be applied. However, for instance in case of strong wave-current interactions, these conditions give not the right description; therefore, the computational grid should be chosen sufficiently large, to avoid disturbances of the wave field in the region of interest.

2.2 THE MODEL HISWA

The model HISWA accounts for refractive propagation of shortcrested waves over arbitrary bottom topography and current fields. The model is based on the action balance equation:

$$(9) \quad \frac{\partial A}{\partial t} + x_i \frac{\partial A}{\partial x_i} + \dot{k}_i \frac{\partial A}{\partial k_i} = T$$

where $A(\vec{k}, \vec{x}, t)$ denotes the wave action density, $x_i \equiv \frac{dx_i}{dt} = \frac{\partial \Omega}{\partial k_i}$ is the group velocity and $\dot{k}_i \equiv \frac{dk_i}{dt} = -\frac{\partial \Omega}{\partial x_i}$ is the rate of change of wave number due to refraction. The right hand side denotes the local change of action density, e.g. by dissipation. The dispersion relation is given as $\omega = \Omega(\vec{k}, \vec{x}, t)$, see (2) and (3). For simplicity we assume in this derivation that there is no ambient current; see Dingemans et al. (1986) for the current case. In the model the simplifying assumption of stationarity, i.e. no explicit dependence on time, is made. Then

Ω is a Hamiltonian for the vectorfield (x_i, k_i) . Transforming from (\vec{k}, \vec{x}) -space to the $(\vec{x}, \omega, \vartheta)$ -space with ϑ the wave direction and introducing the absolute energy density \tilde{E} by $\tilde{E} = A\omega$, one obtains after integration over ω between 0 and ∞ :

$$(10) \quad \frac{\partial}{\partial x} [\omega^A \cdot A^{(o)} \cdot \bar{c}_g \cos\vartheta] + \frac{\partial}{\partial y} [\omega^A \cdot A^{(o)} \cdot \bar{c}_g \sin\vartheta] + \frac{\partial}{\partial \vartheta} [\omega^A \cdot A^{(o)} \cdot \bar{c}_\vartheta] = T_1$$

where the mean quantities ω^A , $A^{(o)}$, \bar{c}_g and \bar{c}_ϑ are defined by:
 $A^{(o)}(x, y, \vartheta) = \int_0^\infty A(x, y, \omega, \vartheta) d\omega$; $\omega^A(x, y, \vartheta) = \frac{1}{A^{(o)}} \int_0^\infty \omega A d\omega$;
 $E^{(o)} = \omega^A \cdot A^{(o)}$; $\bar{c}_g = \frac{1}{E^{(o)}} \int_0^\infty \tilde{E} \cdot c_g d\omega$; $\bar{c}_\vartheta = \frac{1}{E^{(o)}} \int_0^\infty \tilde{E} (c_g - \frac{c}{2}) \frac{1}{h} \frac{\partial h}{\partial n} d\omega$;
 $T_1 = \int_0^\infty \omega T d\omega$; $c_g = \frac{\partial \Omega}{\partial k}$; $c = \frac{\omega}{k}$; $\vec{n} = (-\sin\vartheta, \cos\vartheta)$.

Using Leibniz' rule and rewriting the result, a second equation is obtained:

$$(11) \quad \frac{\partial}{\partial x} [A^{(o)} \cdot \bar{c}_g \cos\vartheta] + \frac{\partial}{\partial y} [A^{(o)} \cdot \bar{c}_g \sin\vartheta] + \frac{\partial}{\partial \vartheta} [A^{(o)} \cdot \bar{c}_\vartheta] = \frac{1}{\omega^A} [T_1 - A^{(o)} \cdot \bar{c}_{g,i} \cdot \frac{\partial \omega^A}{\partial x_i}]$$

Equation (10) and (11) are the basic equations for HISWA. The source term T_1 is implemented as $(\omega^A/\sigma^A) \cdot S^{(o)}$, where $S^{(o)}$ denotes the local chance of energy and $\bar{c}_{g,i} \cdot \frac{\partial \omega^A}{\partial x_i}$ is interpreted as the change of the frequency ω^A , which is prescribed as a function S_ω of the local data.

The source terms $S^{(o)}$ and S_ω represent the effects of wave breaking, bottom friction, wind wave generation, and wave blocking on an opposing current. The dissipation due to wave breaking and bottom friction is modelled by the same methods as used in the CREDIZ model. The formulation is extended to random waves with directional distribution by assuming that the dissipation per direction is proportional to the energy density at that direction. The formulation of the source term for wave generation by wind is based on available expressions giving the total energy and the frequency averaged over the whole spectrum, as functions of fetch and wind speed. Details can be found in Holthuijsen et al. (1988).

The first order partial differential equations (10, 11) can be solved on a regular grid in (x,y,ϑ) -space, with the x-direction parallel to the main direction of the wave field. In the present version of the model, a leapfrog finite difference scheme is used, together with appropriate boundary conditions. As initial conditions, the wave height, period, direction and spreading (or the directional spectrum) of the incident wave field are required.

3. COMPARISON WITH FIELD MEASUREMENTS

The present verification study concerns two field situations:

- the tidal inlet of Texel,
- the estuary of Haringvliet.

Results of the comparison are presented below.

3.1 THE TIDAL INLET OF TEXEL.

This is a strait connecting an ebb tidal delta at the North Sea side with the area of interest, the Wadden Sea, at the other side (see fig. 1). The entrance of the inlet is sheltered by a shoal, which is flooded only during very high tide. The effect of the local wind is thus dominant, while the influence of the tidal current is of secondary importance.

Wave data are available from five locations, of which we used three in this paper:

EIERLAND, located offshore in the North Sea, to provide the input wave conditions for the models;

BOLLEN and MALZWIN, located in the Wadden Sea, to verify the numerical models.

Apart from the wavestaff at MALZWIN, waverider buoys were employed at the measurement locations. Measurements were selected from the period 11 October 1981 to 11 March 1982, using the criteria:

- wind direction ranging from 220° to 300° (\pm SW to NW);
- wind speed higher than 6 m/s.

In table 1 thirteen selected cases are shown which provide the input wave parameters measured at the offshore buoy. In each case, the tidal current is represented by one of four characteristic stages: maximum ebb, slack tide ebb-flood, maximum flood, slack tide flood-ebb (see figs. 2 - 5). The wave direction of the incident wave field is assumed to be equal to the wind direction, given in table 1.

The bottom topography is represented by a depth array of 136×104 grid points, with a spacing of 250 m. At the same grid points, the components of the current velocities are given. Further details can be found in: den Adel (1988). The results of the computations of the models are compared with the measurements in table 1, and a scatter plot is given in fig. 10.

From the computations we draw the conclusions:

- the influence of the local wind is most important in this area: when wave growth due to wind is not accounted for, the computed wave height reduces to values less than a few percent of the incident wave height. This is mainly due to -besides breaking on the shoal- diffraction of wave energy in the Wadden Sea: swell decays here rapidly.
- the influence of the tidal current (with velocities up to 1.5 m/s) can be appreciable: differences of more than 50% may be found, comparing cases

with and without current; in the maximum-ebb case nr. 13, a tunneling of waves does occur (see figs. 6, 7 and 8, 9).

- the influence of the waves on the North Sea is very small; only during maximum-ebb-flow and if the waves come from the South-East more than a few percent of the input wave height remains at the Wadden Sea.
- the change in significant wave period plays a role: at lower periods, the wave-current interaction is stronger, while refraction by depth and bottom friction are weaker. This partially explains the differences in the results of the model computations.

Remarks

1. The present version of the model HISWA does not perform well in case of very small directional distribution; therefore, the model should be used with care when swell-components are present in the wave field.
2. The model CREDIZ shows a sensitive dependence of the side-boundary conditions of the computational grid, in case of strong tidal currents crossing these boundaries; care should be taken that the wave field in the area of interest is not disturbed, by choosing the computational grid sufficiently large.

3.2 THE ESTUARY OF HARINGVLIET.

This area is characterized by a shoal called Hinderplaat which falls partly dry during low tide, a region with nearly straight isobaths offshore the shoal, and a complicated bottom geometry inshore (see fig. 11). In the vicinity of the shoal, wave breaking is the predominant physical process; after this breaking, the wind may enhance the wave height appreciably along a distance of a few miles behind the shoal.

Wave data are available from a measurement campaign during the autumn of 1982 (for details, see Dingemans, 1983; Dingemans et al. 1984). Recently, this data set has been used extensively to test the performance of numerical shallow water wave models (Martin et al. 1987; Vincent and Carrie, 1988). However, energy input from the wind is not included in these models.

In order to test the effect of the local wind, the storm situation of 14 - 15 October 1982 was selected. For a fair comparison with previous CREDIZ results, the same cases as described by Dingemans (1983) were used, with the same input parameters (e.g. the 1981 - bottom topography, consisting of 88 x 117 grid points with spacing of 250 m, and a bottom friction factor $f = 0.005$ instead of the more appropriate 0.01). Further input conditions were:

- wind direction ranging from 300° to 320° ;
- wind speed ranging from 12.9 to 16.5 m/s;
- peak period ranging from 7.1 to 8.3 s (at the Wavec buoy).

The results of the computations are shown in table 2, where the relative error δ is defined by $\delta = (H_s - H_{sm})/H_{sm}$. For each of the six cases, the bias b and the rms-deviation ϵ_{rms} are given in table 3.

By definition, $b = \sum (H_s - H_{sm}) / \sum H_{sm}$;

$$\epsilon_{rms} = [n^{-1} \sum (H_s - H_{sm})^2]^{1/2} / [n^{-1} \sum H_{sm}].$$

The following conclusions may be inferred:

- the model CREDIZ (and, to a lesser extent, also HISWA) performs much better when wave growth due to wind is properly accounted for, especially at low water levels.
- while HISWA performs well at E-75, the wave-staff far behind the shoal, CREDIZ still gives too low values of H_s there; this is probably due to the effect of directional spreading of the wave field, and the transfer of energy between spectral components, resulting in a lowering of the significant wave period, and less dissipation due to bottom friction.
- the computed wave height at WR4, just behind the Hinderplaat, is still too low for low water levels; this is probably due to (local) set-up of the mean water level by waves, which effect is not included in the models.
- at the other locations (mainly at WR5 and WR6), the process of spectral saturation (white-capping) is of importance. This process is simulated in the models by the dissipation method of Battjes and Janssen (1978) for random breaking waves, where breaking is caused also by exceedence of steepness.

4. CONCLUSIONS

A verification study of two wave propagation models has been made, using field data in which the influence of the local wind is significant. In spite of the distinct differences between the models (e.g. CREDIZ is a monochromatic model including diffractive effects, while HISWA is a variable frequency model with directional spreading effects), both models perform equally well in complicated coastal areas. (For specific conclusions, see §3.1 and §3.2).

There remains the problem to describe in a more fundamental way changes in wave frequency, especially in shallow water (for instance, by the undular bore model; see Dingemans and Battjes, these Proceedings). This is important when the models are used in sediment transport studies.

Acknowledgements.

The authors would like to thank J.D. den Adel, J. Hoekema, A.W. Hokke, D. Knoester, T. Louters and A.M. Walburg for assistance in the computations, R.C.M. Ariaans and A.P. Roskam for supplying the field data.

Table 1. Comparison of significant wave heights and periods, Texel.

case nr.	water level (m)	tidal stage	wind speed (m/s)	wind direction (°)	incident wave EIERLAND		wave height (m)			wave period (s)		location
					Hs(m)	Ts(m)	meas.	CREDIZ	HISWA	meas.	HISWA	
1	0.49	ebb-flood	8	250	1.38	6.1	0.15	0.26	0.23	3.7	3.6	BOLLEN
2	0.20	,,	18	270	4.41	10.0	0.86	0.55	0.84	3.8	3.9	,,
3	0.50	,,	18	270	4.41	10.0	0.88	0.74	0.82	3.5	4.0	,,
4	0.52	max. flood	7	280	1.92	9.1	0.14	0.19	0.15	3.6	4.5	,,
5	1.00	,,	9	240	1.35	6.0	0.20	0.27	0.21	4.0	4.0	,,
6	0.87	flood-ebb	7	230	1.12	6.4	0.15	0.15	0.30	3.7	2.6	,,
7	0.12	,,	8	280	1.81	8.2	0.27	0.29	0.26	3.4	2.9	,,
8	1.73	,,	15	280	4.24	9.6	0.64	0.52	0.33	3.6	4.8	MALZWIN
9	1.49	,,	15	280	4.24	9.6	0.55	0.51	0.33	4.2	4.6	,,
10	-0.18	max. ebb	6	290	1.01	6.2	0.30	0.17	0.15	2.8	3.3	BOLLEN
11	-0.62	,,	9	300	1.69	7.7	0.21	0.29	0.35	3.4	2.6	,,
12	-0.48	,,	9	220	2.28	7.0	0.51	0.28	0.32	3.3	5.3	,,
13	-0.43	,,	11	230	2.24	7.7	0.36	0.38	0.38	4.7	4.7	,,

Table 2. Comparison of significant wave heights, Haringvliet.

date and time	water level	location	measurement		CREDIZ (new)		HISWA (new)	
			H _{sm}	H _s	H _s	$\delta(\%)$	H _s	$\delta(\%)$
82 10 14 17:00	-0.10	Wa	2.58	2.58	2.58	0	2.58	0
		WR1	2.34	2.55	+9	2.58	+10	
		WR2	2.21	2.31	+5	2.34	+6	
		WR3	2.21	2.23	+1	2.30	+4	
		WR4	0.40	0.29	-27	0.28	-30	
		WR5	0.66	0.76	+15	0.89	+35	
82 10 14 20:00	0.20	WR6	1.16	1.29	+11	1.22	+5	
		E-75	0.61	0.52	-15	0.58	-5	
		Wa	3.06	3.06	0	3.06	0	
		WR1	2.65	2.98	+12	3.05	+15	
		WR2	2.38	2.57	+8	2.56	+8	
		WR3	2.45	2.48	+1	2.50	+2	
82 10 14 22:00	0.85	WR4	0.48	0.33	-31	0.36	-25	
		WR5	0.75	0.89	+19	1.00	+33	
		WR6	1.20	1.39	+16	1.32	+10	
		E-75	0.74	0.46	-38	0.64	-14	
		Wa	3.23	3.23	0	3.23	0	
		WR1	2.90	3.18	+10	3.24	+12	
82 10 14 23:00	0.45	WR2	2.53	2.85	+13	2.83	+12	
		WR3	2.70	2.74	+1	2.77	+3	
		WR4	0.62	0.52	-16	0.65	+5	
		WR5	1.05	1.17	+11	1.21	+15	
		WR6	1.60	1.61	+1	1.56	-3	
		E-75	0.94	0.78	-17	0.86	-9	

Table 2. Continued

date and time	water level	location	measurement		CREDIZ (new)		HISWA (new)	
			H _{sm}	H _s	H _s	$\delta(\%)$	H _s	$\delta(\%)$
82 10 14 23:00	1.70	Wa	3.54	3.54	0	3.54	0	
		WR1	3.10	3.40	+10	3.54	+14	
		WR2	2.63	3.11	+18	3.16	+20	
		WR3	2.72	3.04	+12	3.11	+14	
		WR4	0.72	0.79	+10	0.99	+38	
		WR5	1.45	1.50	+3	1.53	+6	
82 10 15 02:00	1.50	WR6	1.86	1.88	+1	1.88	+1	
		E-75	1.08	0.99	-8	1.10	+2	
		Wa	2.89	2.89	0	2.89	0	
		WR1	2.68	2.82	+5	2.86	+7	
		WR2	2.75	2.70	-2	2.83	+3	
		WR3	2.68	2.74	+2	2.81	+5	
82 10 15 04:00	0.45	WR4	0.70	0.76	+9	0.88	+26	
		WR5	1.15	1.39	+21	1.40	+22	
		WR6	1.95	1.63	-16	1.75	-10	
		E-75	0.88	0.46	-48	1.05	+19	
		Wa	2.72	2.72	0	2.72	0	
		WR1	2.49	2.63	+6	2.72	+9	
82 10 15 06:00	0.45	WR2	2.41	2.43	+1	2.53	+5	
		WR3	2.56	2.44	-5	2.49	-3	
		WR4	0.44	0.30	-32	0.44	0	
		WR5	0.70	0.99	+41	1.05	+50	
		WR6	1.35	1.32	-2	1.40	+4	
		E-75	0.63	0.50	-21	0.72	+14	

Table 3. Bias and rms-deviation (%); Haringvliet.

time	water level (m)	CREDIZ, <u>old</u> *)		CREDIZ, <u>new</u>		HISWA, <u>new</u>	
		b	ϵ_{rms}	b	ϵ_{rms}	b	ϵ_{rms}
17.00	- 0.10	- 1.5	19.2	+ 3.8	8.8	+ 6.3	10.8
20.00	0.20	- 2.4	26.1	+ 4.2	13.7	+ 7.3	13.5
22.00	0.85	+ 1.9	16.5	+ 4.1	10.3	+ 6.3	10.6
23.00	1.70	+ 6.9	12.4	+ 8.5	12.9	+12.9	16.4
02.00	1.50	- 3.2	15.3	- 2.3	12.5	+ 6.2	9.7
04.00	0.45	+ 0.5	13.4	+ 0.3	9.9	+ 7.3	11.3

*) Cf. Dingemans et al. (1984)

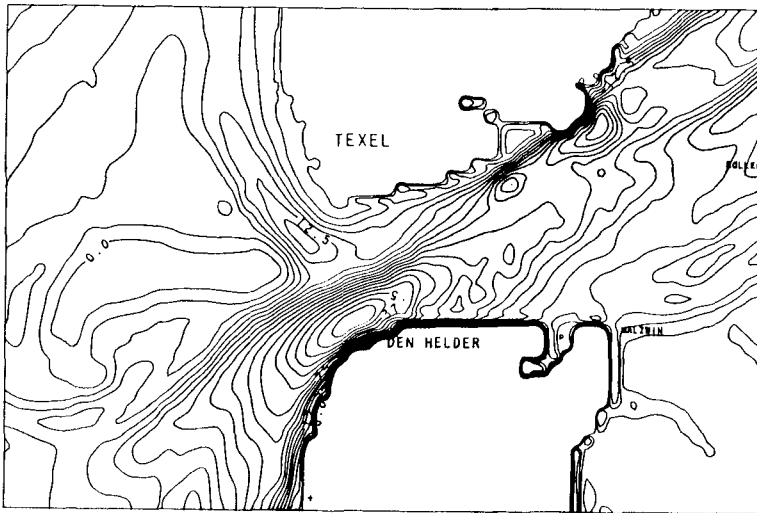


Fig. 1 Bottom contours, tidal inlet of Texel.

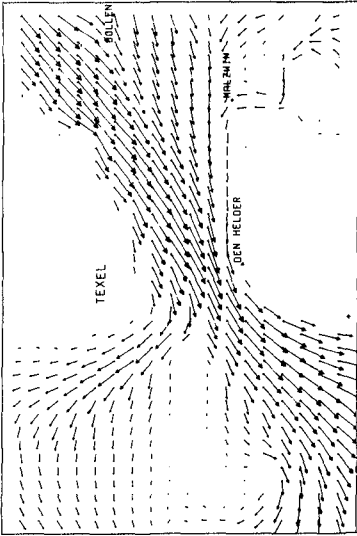


Fig. 2 Maximum ebb current.

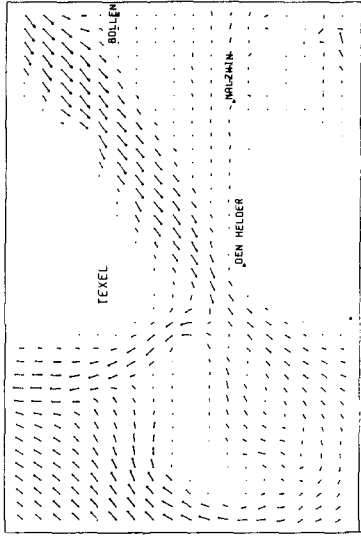


Fig. 3 Slack tide ebb-flood current.

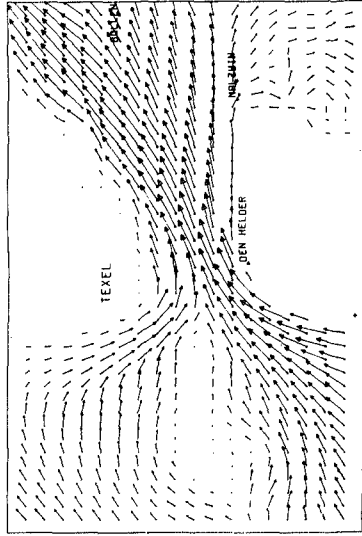


Fig. 4 Maximum flood current.

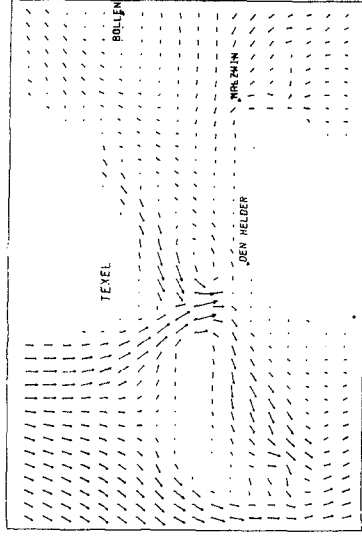


Fig. 5 Slack tide flood-ebb current.

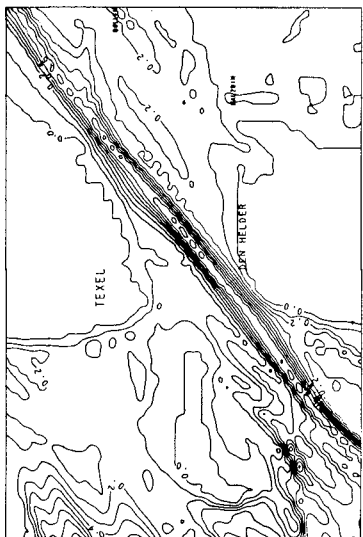


Fig. 6 Isolines of amplitude (CREDIZ), max. ebb current.

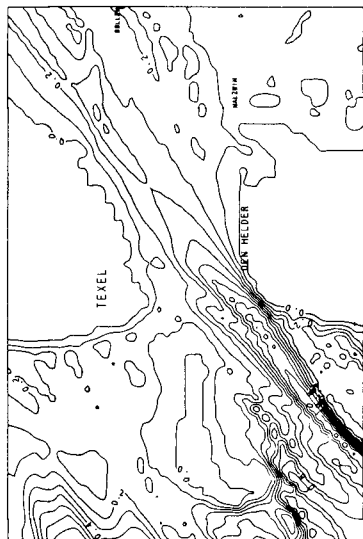


Fig. 7 Isolines of amplitude (CREDIZ), no current.

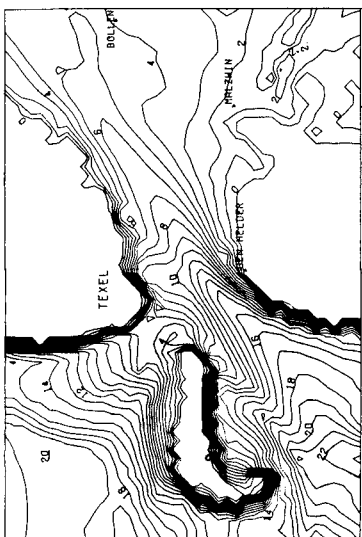


Fig. 8 Isolines of wave height (HISWA), max. ebb current.

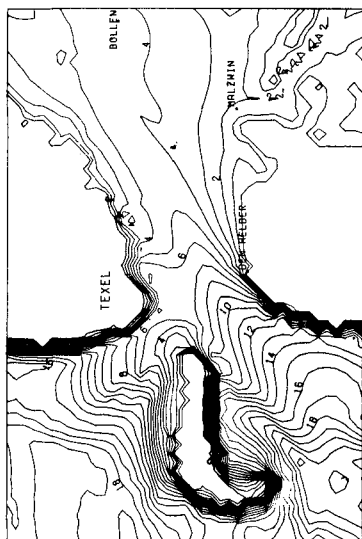


Fig. 9 Isolines of wave height (HISWA), no current.

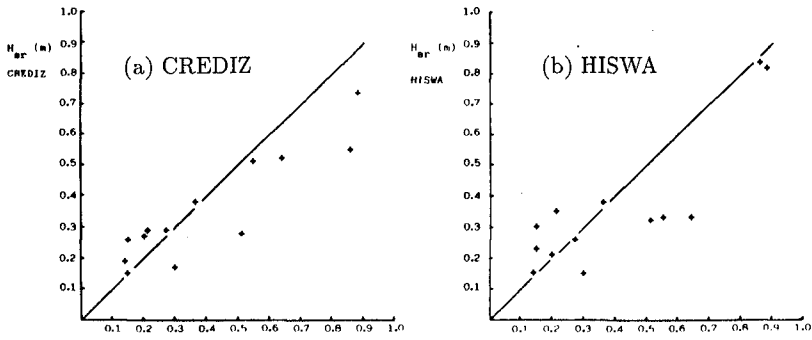


fig. 10 Comparison of measured and computed wave heights.

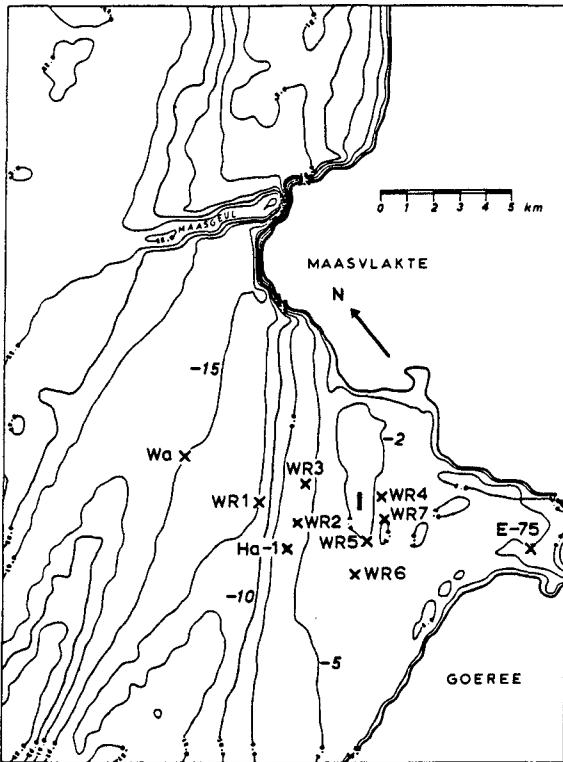


Fig. 11 Bottom contours, estuary of Haringvliet.

REFERENCES

- Adel, J.D. den, *Verificatie van de numerieke golfvoortplantingsmodellen CREDIZ en HISWA bij het zeegat van Texel*, Rijkswaterstaat, Report GWAO 88.044 (in Dutch) (1988).
- Battjes, J.A. and Janssen, J.P.F.M., *Energy loss and set-up due to breaking of random waves*, Proc. 16th Coastal Eng. Conf. ASCE, Hamburg, 569 - 587 (1978).
- Battjes, J.A. and Stive, M.J.F., *Calibration and verification of a dissipation model for random breaking waves*, J. Geophys. Res. 90 (C5), 9159 - 9167 (1985).
- Dingemans, M.W., *Verification of numerical wave propagation models with field measurements. CREDIZ verification Haringvliet*, Delft Hydraulics Lab., Report W 488 (1983).
- Dingemans, M.W., *Surface wave propagation over an uneven bottom. Evaluation of two-dimensional horizontal wave propagation models*, Delft Hydraulics Lab., Report W 301, part 5 (1985).
- Dingemans, M.W.; Stive, M.J.F.; Kuik, A.J.; Radder, A.C. and Booij, N., *Field and Laboratory verification of the wave propagation model CREDIZ*, Proc. 19th Coastal Eng. Conf. ASCE, Houston, 1178 - 1191 (1984).
- Dingemans, M.W.; Stive, M.J.F.; Bosman, J.; De Vriend, H.J. and Vogel, J.A., *Directional nearshore wave propagation and induced currents*, Proc. 20th Coastal Eng. Conf. ASCE, Taipei, 1092 - 1106 (1986).
- Holthuijsen, L.H., *Methoden voor golfvoorspelling (in Dutch)*, Technische Adviescommissie voor de Waterkeringen (1980).
- Holthuijsen, L.H. and Booij, N., *A grid model for shallow water waves*, Proc. 20th Coastal Eng. Conf. ASCE, Taipei, 261 - 270 (1986).
- Holthuijsen, L.H.; Booij, N. and Herbers, T.H.C., *A prediction model for stationary, short-crested waves in shallow water with ambient currents*, Coastal Engineering, in preparation (1988).
- Krylov, Yu.M. Strelakov, S.S. and Tsyplukhin, V.F., *Vetrovye volny i ich vozdejstvie na sooruzewija (wind waves and their impact on structures). In Russian*, Hydrometeoizdat, Leningrad (1976).
- Martin, C.J.; Dalrymple, R.A. and Miller, M.C., *A verification procedure for wave propagation models*, Modelling the Offshore Environment, Proc. of an international conference, Society for Underwater Technology, London. Chap. 13, 181 - 202 (1987).
- Putnam, J.A. and Johnson, J.W., *The dissipation of wave energy by bottom friction*, Transactions Am. Geophys. Union, 30, 67 - 74 (1949).
- Radder, A.C., *On the parabolic equation method for water wave propagation*, J. Fluid Mech. 95, 159 - 176 (1979).
- Vincent, C.E. and Carrie, A., *Evaluation of an energy propagation wave refraction model*, Continental Shelf Res. 8 (3), 287 - 305 (1988).
- Wilson, B.W., *Numerical prediction of ocean waves in the North Atlantic for December, 1959*, Deutsche Hydrographische Zeitschrift, 18 (3), 114 - 130 (1965).